IET Generation, Transmission & Distribution

Research Article

IET Journals
The Institution of Engineering and Technology

Wide range algorithm for directional earth-fault protection without voltage inputs

ISSN 1751-8687
Received on 1st July 2019
Revised 25th February 2020
Accepted on 20th April 2020
E-First on 20th May 2020
doi: 10.1049/iet-gtd.2019.0763
www.ietdl.org

Zoran N. Stojanović[1], Mileta D. Žarković[1] ✉

[1]*Department of Power Systems, School of Electrical Engineering, University of Belgrade, Bulevar kralja Aleksandra 73, Belgrade, Serbia*
✉ *E-mail: mileta@etf.rs*

Abstract: In this study, algorithm for a directional earth-fault relay is modified to work properly without voltage inputs. The presented modification of the algorithm implies that only current inputs are required, and the algorithm is used in isolated neutral networks. The main modification of this algorithm is that only one phase current is used as a reference quantity instead of the zero sequence voltage or three phase currents. The algorithm is further upgraded by using the phase current of the supply feeder as a reference signal for all relays of outgoing feeders. This way the reference quantity becomes more stable and the number of measurements per feeder is reduced to only one. The introduction of simple communication between relays on feeders, a wide operation range is achieved. With this algorithm detection of earth-fault is ensured regardless of the network load: purely capacitive, predominantly resistive or purely inductive. The algorithm successfully detects the faulted line and phase containing a phase-to-earth fault. The aim of this study is to design low-cost directional relays with no voltage inputs, a small number of current measurements and a wide range of possible network loads.

1 Introduction

The medium voltage industrial and distribution networks are usually realised as isolated neutral networks. In these networks, upon the appearance of a phase-to-earth fault, the fault current does not exceed 30 A [1]. Therefore, the functioning of the system can be continued without any interruption. However, since there is a risk of appearance of a second phase-to-earth fault in one of the healthy phases, it is important that the first phase-to-earth fault is detected and removed. As in networks with isolated neutral point the earth fault current closes through phase-to-earth capacitances of faulted lines, but also of all other (healthy) lines, for gaining selective protection it is necessary to employ directional earth fault protection in spite of the fact that the network is radial. Conventional solutions require zero-sequence voltage measurement in order to determine the direction of the earth-fault current.

The directional element appears in several types of protections (overcurrent, differential, distance etc.) as an additional function which provides selectivity of protection. Its function is to determine the direction of the measured current with respect to a reference quantity and this is based on the phase shift between those two values. Reference quantity can be either voltage or some other current. Phase shifts between electrical variables can be determined by various methods. In the case of transmission lines for high or extremely high voltage, the method based on increments of instantaneous electrical values or the travelling wave method are applied [2, 3]. When there is no need for a fast response, the methods based on vectors of electrical quantities [4] or on their increments [2, 5] are used. In order to determine the amplitude and initial phase angle, some of the well-known methods of signal processing are available, such as: zero-crossing [6], Fourier's method [7], least error squares [8], Newton's method [9] etc. The direction can be found based on the integral of the instantaneous signal power without calculating the phase and this protocol is described in [10]. Some new algorithms, which optimise directional overcurrent relay in power distribution systems, are using genetic algorithm [11] or teaching learning-based optimisation [12, 13].

In some specific cases, for determination of the fault direction, it is possible to use only current inputs. Therefore, for the parallel transmission lines, directional transverse differential protection could be carried out by the comparison of increments of the current sample magnitudes [14]. The improved solution which, in addition to magnitudes, considers phase angles of line currents is given in [15]. As the direction of the pre-fault current in the lines, which connect power plant with the network, is known in advance, this current can be used as a reference quantity for determination of fault direction [16]. In [17], a new directional algorithm is proposed, which can detect faults direction using the only sign of the imaginary part of the post-fault current phasor. The article by Costa *et al*. [18] explains how directional relays should be coordinated to operate as fast as possible and in the adequate sequence. In relation to all papers, the review paper [19] presents the state-of-the-art technologies and techniques for determining single-phase earth fault location on distribution networks.

In medium voltage industrial networks phase currents slightly vary upon a phase-to-earth fault occurrence and these currents can be used as reference quantities instead of the zero-sequence voltage. The idea and algorithm were published in [20]. Improved algorithm [21] uses only one phase current instead of three phase currents. This way, the absolute phase and amplitude symmetry of the reference value is achieved. Also, the required number of measurements is reduced from 4 to 2 per feeder. However, both algorithms [20, 21] have the same limitation: a load of the feeders must be known in a range of 60°. In case of exceeding the predefined range, the relay will make mistakes. This study presents a solution to the described problem, by which the relay operating range is extended from the mentioned 60°–120°. This way directional earth-fault relay without voltage inputs can be used in purely capacitive, predominantly resistive or purely inductive networks.

This study is organised as follows: Section 2 presents the existing algorithms for directional earth-fault protection without voltage inputs. Section 3 presents explanation on how the algorithm works in network with load range extension, with pure capacitive or pure inductive load. Section 4 presents testing of the algorithm with a discussion on the obtained results. Conclusions are presented in Section 5.

2 Existing algorithms for directional earth-fault protection without voltage inputs

The algorithm which uses three phase currents instead of zero sequence voltage is described in [20]. Four measurements are used

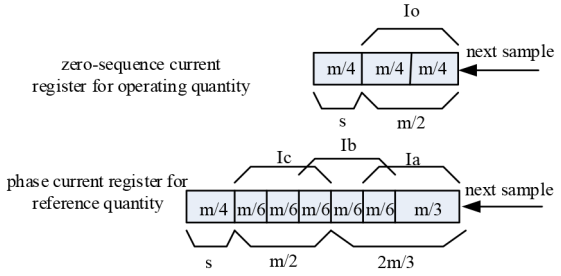

Fig. 1 *Example of current registers*

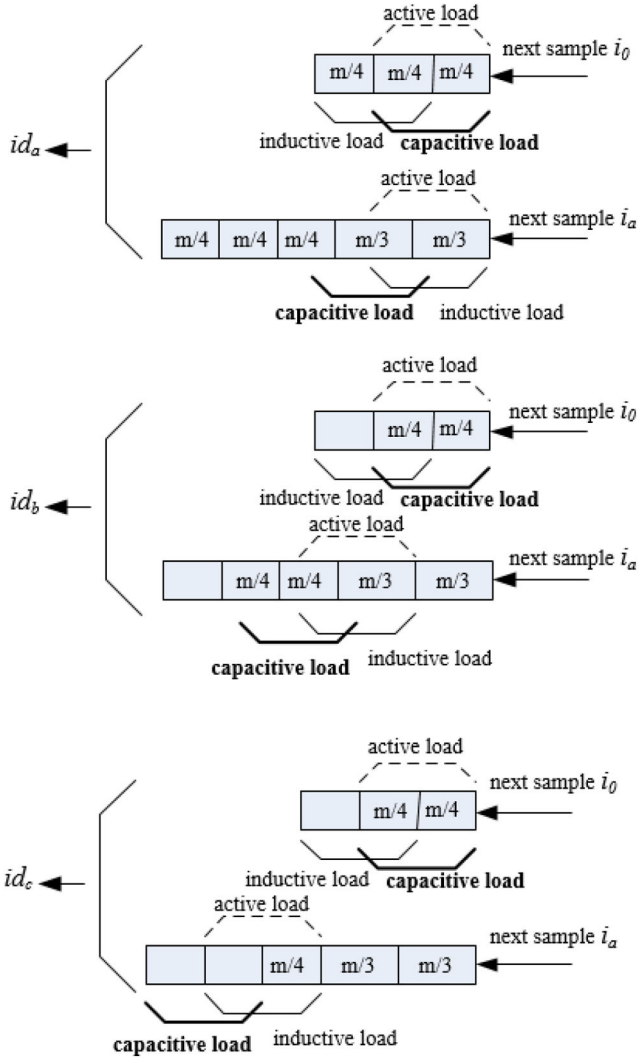

Fig. 2 *Sensitivity adjustment for different type of loads*

in this algorithm: three phase currents i_a, i_b and i_c as reference quantities and zero component of current i_0 as an operating quantity. Each variable is stored in register, length of $3m/4$ samples (m – number of samples per basic period). The half of m samples requires an instantaneous power integral and a mean value method. One quarter of m samples are used for setting sensitivity of the algorithm. Without setting the sensitivity ($s = 0$), the algorithm effectively recognises the earth-fault for the load range between 0° and 60°. If we want to shift the load range of 60° to capacitive loads, then the sensitivity s should be set to a value >0. If we want to shift the load range of 60° to extremely inductive loads, then the sensitivity s should be set to a value <0.

For predominantly resistive loads, the sensitivity s (>0) is located in the phase currents registers. The direction indicators in phases a, b and c are calculated as

$$\mathrm{id}_{a,b,c} = \frac{4m}{\pi^2} \cdot \frac{\sum_{k=m/4+1}^{3m/4} i_{a,b,c}(k-s) i_0(k)}{\sum_{k=m/4+1}^{3m/4} |i_{a,b,c}(k-s)| \sum_{k=m/4+1}^{3m/4} |i_0(k)|} \quad (1)$$

where: $i_{abc}(k)$ indicates phases current samples, $i_o(k)$ indicates samples of the zero-sequence current.

For extremely inductive loads, the sensitivity s (<0) is located in zero-sequence current register. The direction indicators are calculated by formula:

$$\mathrm{id}_{a,b,c} = \frac{4m}{\pi^2} \cdot \frac{\sum_{k=m/4+1}^{3m/4} i_{a,b,c}(k) i_0(k+s)}{\sum_{k=m/4+1}^{3m/4} |i_{a,b,c}(k)| \sum_{k=m/4+1}^{3m/4} |i_0(k+s)|} \quad (2)$$

Described methodology was improved using only one phase current [21]. Indicator of the direction of the other two phases is calculated using the same current, previously shifted for $2\pi/3$ rad ($m/3$ samples) and $4\pi/3$ rad ($2m/3$ samples). Because of the required phase shifting, register of the phase current is extended with 2 $m/3$ samples (Fig. 1).

For achieving phase symmetry m needs to be dividable by 3. Otherwise phase shift between I_a and I_b and I_c will not be $2\pi/3$ rad. Also, m must be dividable by 2 because $m/2$ samples are used for calculating integral of the instantaneous power and mean value method. Finally, number of samples per signal period m must be dividable by 6.

Based on previous discussion, id in the dominantly resistive loaded network takes the form ($s > 0$)

$$\mathrm{id}_a = \frac{4m}{\pi^2} \cdot \frac{\sum_{k=m/4+1}^{3m/4} i_a(k+2m/3-s) i_0(k)}{\sum_{k=m/4+1}^{3m/4} |i_a(k+2m/3-s)| \sum_{k=m/4+1}^{3m/4} |i_0(k)|}, \quad (3)$$

$$\mathrm{id}_b = \frac{4m}{\pi^2} \cdot \frac{\sum_{k=m/4+1}^{3m/4} i_a(k+m/3-s) i_0(k)}{\sum_{k=m/4+1}^{3m/4} |i_a(k+m/3-s)| \sum_{k=m/4+1}^{3m/4} |i_0(k)|}, \quad (4)$$

$$\mathrm{id}_c = \frac{4m}{\pi^2} \cdot \frac{\sum_{k=m/4+1}^{3m/4} i_a(k-s) i_0(k)}{\sum_{k=m/4+1}^{3m/4} |i_a(k-s)| \sum_{k=m/4+1}^{3m/4} |i_0(k)|} \quad (5)$$

when the network is dominantly inductive loaded next formulas should be used ($s < 0$)

$$\mathrm{id}_a = \frac{4m}{\pi^2} \cdot \frac{\sum_{k=m/4+1}^{3m/4} i_a(k+2m/3) i_0(k+s)}{\sum_{k=m/4+1}^{3m/4} |i_a(k+2m/3)| \sum_{k=m/4+1}^{3m/4} |i_0(k+s)|}, \quad (6)$$

$$\mathrm{id}_b = \frac{4m}{\pi^2} \cdot \frac{\sum_{k=m/4+1}^{3m/4} i_a(k+m/3) i_0(k+s)}{\sum_{k=m/4+1}^{3m/4} |i_a(k+m/3| \sum_{k=m/4+1}^{3m/4} |i_0(k)+s|}, \quad (7)$$

$$\mathrm{id}_c = \frac{4m}{\pi^2} \cdot \frac{\sum_{k=m/4+1}^{3m/4} i_a(k) i_0(k+s)}{\sum_{k=m/4+1}^{3m/4} |i_a(k| \sum_{k=m/4+1}^{3m/4} |i_0(k)+s|} \quad (8)$$

Fig. 2 presents which samples are used for calculating indicators id_a, id_b and id_c for different type of loads.

The advantage of the algorithm [21] is the absolute phase and amplitude symmetry of the reference value, which was kept by artificial shifting of the measured phase current. In the case of using the original phase currents [20], this symmetry would be impaired due to the impact of fault currents. Also, in isolated neutral networks two-phase overcurrent protection is often used instead of three-phase overcurrent protection because of economic reasons and better selectivity in case of double earth-fault. In such cases, the improved algorithm [21] solves the problem of missing phase current measurement. Tripping conditions of both algorithms are the same and are given in Table 1, column 2.

Table 1 Tripping condition for fault in different phases

Phase fault	Tripping condition	Tripping condition capacitive load	Tripping condition inductive load
A	$id_a < 0$ & $id_b < 0$ & $id_c > 0$	$id_a > 0$ & $id_b < 0$ & $id_c < 0$	$(n-1)$ indicates $B \rightarrow A$ of unexcited relay
B	$id_a > 0$ & $id_b < 0$ & $id_c < 0$	$id_a < 0$ & $id_b > 0$ & $id_c < 0$	$(n-1)$ indicates $C \rightarrow B$ of unexcited relay
C	$id_a < 0$ & $id_b > 0$ & $id_c < 0$	$id_a < 0$ & $id_b < 0$ & $id_c > 0$	$(n-1)$ indicates $A \rightarrow C$ of unexcited relay

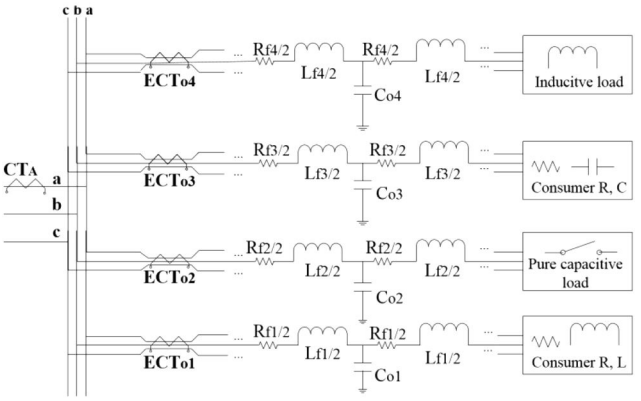

Fig. 3 *Test distribution network with specified measuring points*

3 Range extension of the algorithm for directional earth-fault protection without voltage inputs

The main limitation of the technique described in [18, 19] is correct operation with a load range of 60°. In other words, the character of the load must be approximately known in advance. If the real load is out of the assumed range, there will be a wrong relay tripping.

Such situations may occur when the feeder with predominantly resistive load becomes predominantly inductive loaded (for example asynchronous motor in idle running) or becomes predominantly capacitive loaded (for example feeder in open circuit).

This limitation can be simply eliminated by bringing a phase current of supply feeder into the directional relay. The reference quantity is thereby more stable and less dependent on a load of individual outgoing feeders. This way, the number of measurements per feeder is reduced to one. This solution will work in the case of predefined working conditions of the incoming (supply) feeder, for example, in dominantly resistive load between −15° and 45°, and then, it is not important if individual outgoing feeders are: capacitive, resistive or inductive. However, in a case when the whole system is working in a dominantly inductive or capacitive regime, i.e. beyond of the assumed range $15° \leq \varphi \leq 45°$, wrong tripping of the relay will occur. Therefore, these two cases will be discussed in more details.

3.1 Pure capacitive load

Test network with one supply feeder and four outgoing feeders is shown in Fig. 3. The zero sequence current of outgoing feeders is measured by the current transformers ECT_0, and phase current of supply feeder is measured by CT_A.

Rare, but the possible situation is that all outgoing feeders are opened. In this case, all phase currents of outgoing feeders are capacitive, and their phasors are 90° ahead of the voltage phasors. Phase current of supply feeder, I_A, is equal to the sum of the phase currents, $I_{a1,2,3,4}$ of outgoing feeders. According to that, Fig. 4*a* shows the phasor of I_a and I_A as parallel. For a fault in phase A of line No. 1, the zero-sequence current phasor diagram is shown in Fig. 4*a*, as well.

Based on phasor diagram shown in Fig. 4*a* marker id of line No. 1 takes the following values: $id_{a1} = \cos(0°) > 0$, $id_{b1} = \cos(-120°) < 0$, $id_{c1} = \cos(120°) < 0$. The zero-sequence currents $I_{02,3,4}$, for the same fault, but seen at the measuring site of health outgoing feeders are shown also in Fig. 4*a*. As can be seen, zero-sequence currents $I_{02,3,4}$, in comparison to the faulted feeder, have the opposite directions. Since the markers of line Nos. 2, 3 and 4 have the following values: $id_{a2,3,4} = \cos(180°) < 0$, $id_{b2,3,4} = \cos(60°) > 0$, $id_{c2,3,4} = \cos(-60°) > 0$. Based on tripping conditions from Table 1-column 2, phase B of outgoing feeder 1 is faulted (B_1). So, the exact defective outgoing feeder is found, but the phase is wrong.

Similar concept holds for faults in phases B (Fig. 4*c*) and C (Fig. 4*e*) of line 1, when marker id takes the following values: $id_{a1} < 0$, $id_{b1} > 0$, $id_{c1} < 0$ and $id_{a1} < 0$, $id_{b1} < 0$, $id_{c1} > 0$, respectively. Using conditions from Table 1-column 2, again there is wrong detection of faulted phase: in the case of fault in phase B algorithm will show fault in phase A and in the case of fault in phase C, algorithm will show fault in phase B.

Based on previous analysis, to detect the faulted phase correctly, tripping conditions from column 2 must be changed to column 3. As a criterion for the automatic change of tripping conditions, the simplest way is introducing the condition $I_A \leq I_{\min}$ (where $I_{\min}$ is some predefined value), because capacitive regime is accompanied by small idle current. $I_{\min}$ should be selected so it is slightly higher than the idle current of the whole network.

It should be emphasised that in the case of a fault from idle operation, the phase current may be of the same order of magnitude as the earth-fault current and therefore the initial assumption of a small change of the phase current during the fault is incorrect. In this situation, it is better to use all three phase currents as reference values [20], instead of only one [21], because the influence of the earth-fault current in such case is distributed on all three phases.

3.2 Pure inductive load

For pure inductive load all the phase currents, of outgoing and supply feeders, are late 90° with respect to the phase voltage. For a fault in phase A of line No. 1, the zero-sequence current phasor diagram is shown in Fig. 4*b*.

Based on phasor diagram shown in Fig. 4*b*, marker id takes the following values: $id_{a1} = \cos(180°) < 0$, $id_{b1} = \cos(-60°) > 0$, $id_{c1} = \cos(60°) > 0$. For these values of markers, based on column 2 of Table 1, line 1 is not faulted. The phasors of electrical values for the same fault, but seen at the measuring site of healthy feeders, are also shown in Fig. 4*b*. Indicators now obtain the following values: $id_{a2,3,4} = \cos(0°) > 0$, $id_{b2,3,4} = \cos(120°) < 0$, $id_{c2,3,4} = \cos(-120°) < 0$. Based on tripping conditions from Table 1, column 2, phase B of outgoing feeders 2, 3 and 4 are faulted. Therefore, instead of A_1, tripping conditions indicate faults in healthy feeders B_2, B_3 and B_4. Similarly, for a fault in phase B of line 2 (Fig. 4*d*), the results of the algorithm would be C_1, C_3 and C_4. For a fault in phase C of line 3 (Fig. 4*f*), the results of the algorithm are A_1, A_2 and A_4.

Based on previous discussion it can be concluded that the algorithm for a fault in phase A shows phase B of healthy feeders, for a fault in phase B shows phase C of healthy feeders and for a fault in phase C shows phase A of healthy feeders. In this case, simple communication between relays resolves the problem. If $n-1$ relays indicate a fault in phase A (n is number of outgoing feeders) then the fault is in the phase C of outgoing feeder where a fault is not indicated. If $n-1$ relays indicate a fault in phase B than the fault is in the phase A of outgoing feeder where a fault is not indicated. Similarly, if $n-1$ relays indicate a fault in phase C than the fault is in the phase B of outgoing feeder where a fault is not indicated. These conditions are shown in column 4 of Table 1.

Established communication neutralises the wrong tripping for dominantly inductive load and thus widens the range of correct directional relay tripping from 60° to 120°. Necessary condition for this solution is the existence of more than two outgoing feeders.

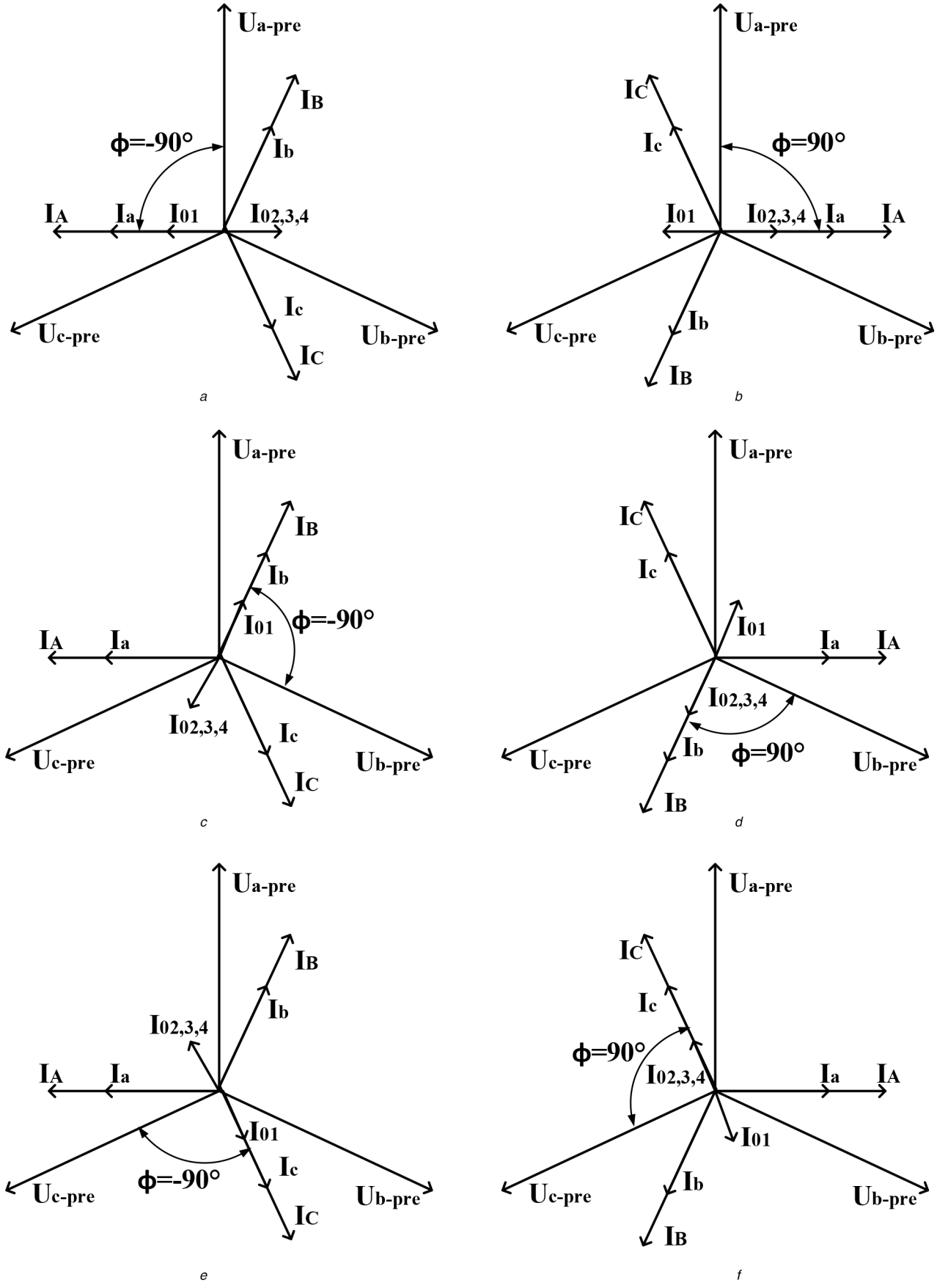

Fig. 4 *Phasor diagrams for a fault in phase A of line no. 1 in distribution network with*
(a) Pure capacitive load, ***(b)*** Pure inductive load; phasor diagrams for a fault in phase B of line no. 1 with, ***(c)*** Pure capacitive load, ***(d)*** Pure inductive load, phasor diagrams for a fault in phase C of line no. 1, ***(e)*** Pure capacitive load, ***(f)*** Pure inductive load

Flow chart of wide range algorithm for directional earth-fault protection without voltage inputs is shown in Fig. 5.

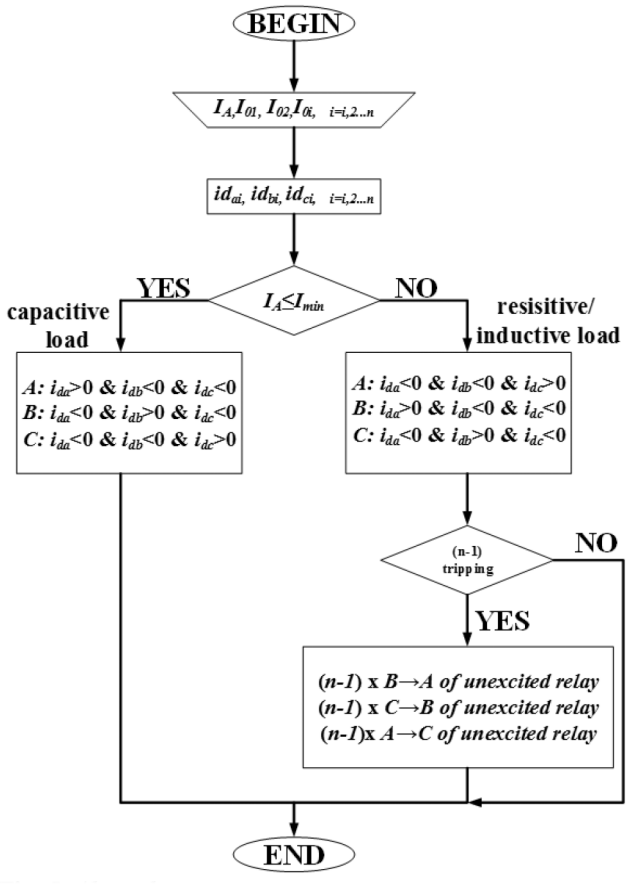

Fig. 5 *Algorithm*

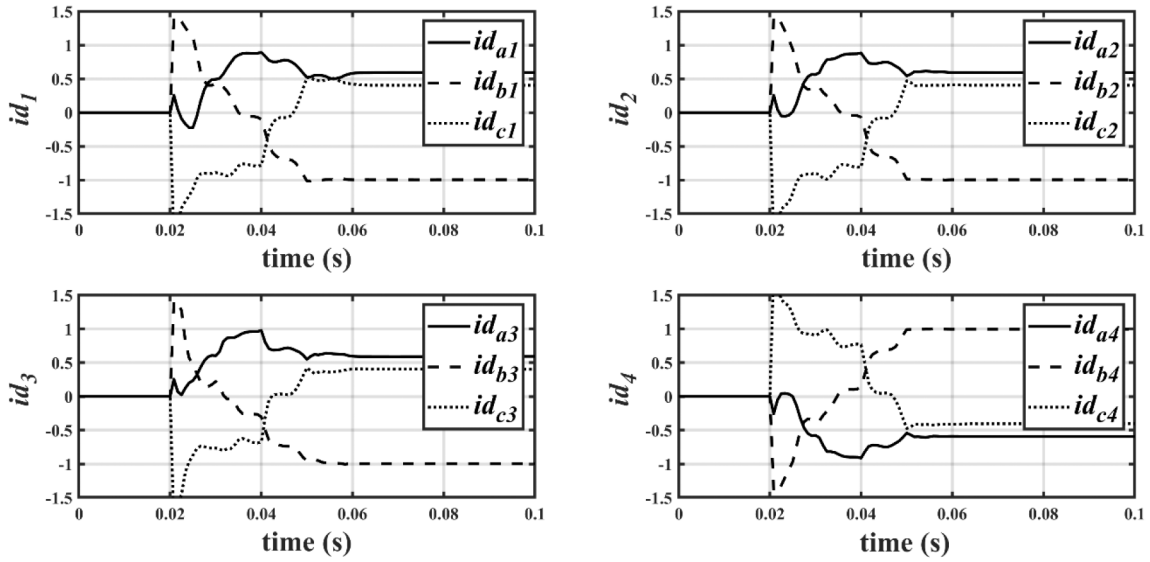

Fig. 6 *The algorithm results for a fault in phase C of line no. 4*

4 Testing the algorithm

The proposed algorithm is tested under different types of load situations of the network model presented in Fig. 2. Different network load situations have been achieved with four different loads: predominantly resistive, predominantly inductive, predominantly capacitive and pure capacitive load (opened feeder). The parameters of the network model (Fig. 2) are: $V_a = V_b = V_c = 10/\sqrt{3}$ kV, $R_{f1} = 0.3\ \Omega$, $L_{f1} = 0.6$ mH, $C_{01} = 1\ \mu$F, $R_{p1} = 25\ \Omega$, $L_{p1} = 28$ mH ($\cos\varphi_1 = 0.94$), $R_{f2} = 0.4\ \Omega$, $L_{f2} = 0.9$ mH, $C_{02} = 1.5\ \mu$F, $R_{f3} = 0.35\ \Omega$, $L_{f3} = 0.7$ mH, $C_{03} = 1.25\ \mu$F, $R_{p3} = 21\ \Omega$, $C_{p3} = 1.08$ mF ($\cos\varphi_3 = 0.99$ capacitive), $R_{f4} = 0.45\ \Omega$, $L_{f4} = 0.8$ mH, $C_{04} = 1.3\ \mu$F, $R_{p4} = 24\ \Omega$ and $L_{p4} = 0.5$ H ($\cos\varphi_4 = 0.15$ inductive).

Sampling frequency was set to $f_s = 1200$ Hz. After sampling, signals were filtered by the cosine Fourier series. Sensitivity s was set to 1 indicating operating range between −15° and 105°. Each simulation takes 0.1 s. Various values of the fault resistance and fault instant are used in simulations in order to investigate the transition period.

In the first simulation a fault in phase C of line no. 4 was made. A fault instant is T ($T = 20$ ms) and R_f (fault resistance) is 0. By applying the described algorithm, the estimation of indicator id is shown in Fig. 6. Since $id_{b4} > 0$, while $id_{a4} < 0$ and $id_{c4} < 0$, the algorithm successfully detects faulted line and phase C_4 (line no. 4, phase C).

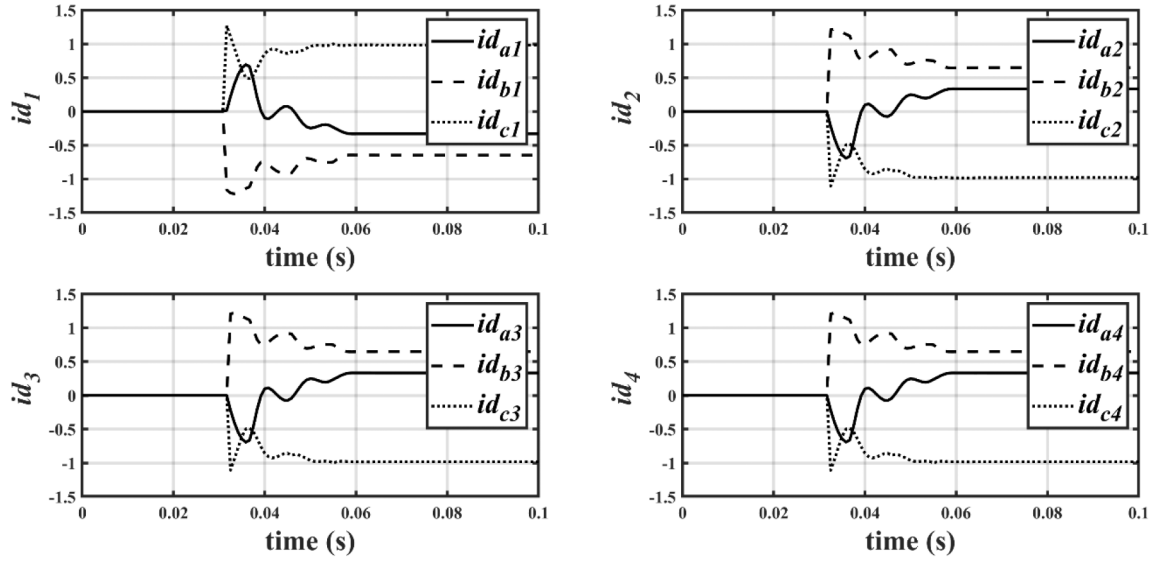

Fig. 7 *Algorithm results for a fault in phase A of line no. 1*

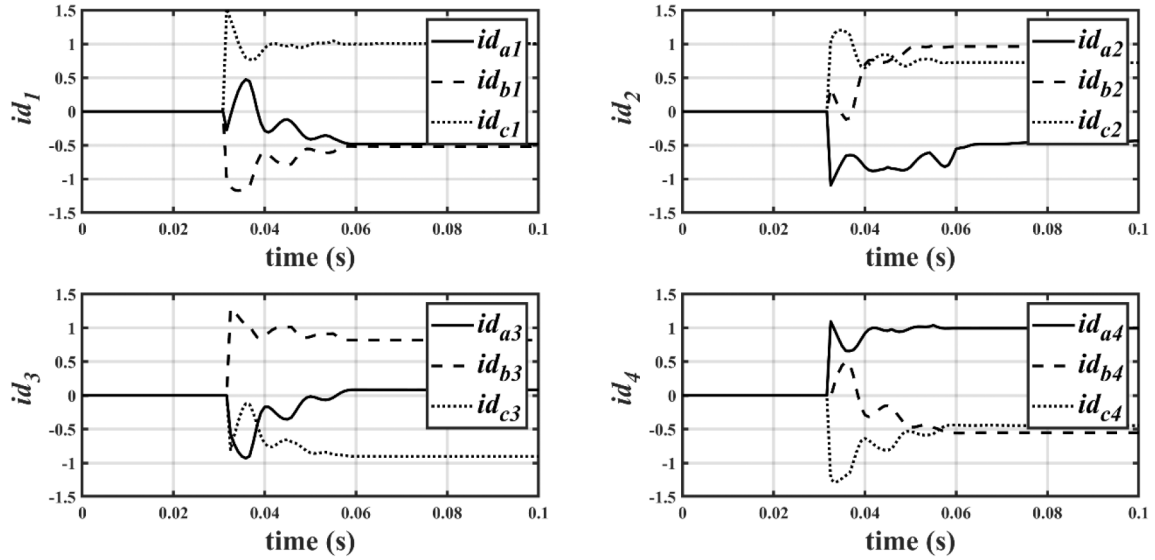

Fig. 8 *Algorithm results for a fault in phase A of line no. 1 using [20, 21]*

The same model is applied for a fault on the first feeder with mainly active load A_1 (line no. 1, phase A). A fault instant is $3T/2$ (30 ms) and R_f is set to 10 Ω. It can be seen from Fig. 7 that the appropriate conditions are satisfied: $\mathrm{id}_{c1} > 0$, $\mathrm{id}_{a1} < 0$ and $\mathrm{id}_{b1} < 0$. The same test is performed with algorithms described in [20, 21]. Based on the results shown in Fig. 8, it can be concluded that the relay 4 will incorrectly signal the fault in the B phase, since $\mathrm{id}_{a4} > 0$, $\mathrm{id}_{b4} < 0$ and $\mathrm{id}_{c4} < 0$. This occurs because algorithms described in [20, 21] as a reference value use phase current of the feeder which is in this specific case predominantly inductive and it is outside of the assumed range, from −15° to 45°, for which the mentioned algorithms operate correctly. The false tripping of relay 4 would occur in other two tests as well for the same reason as in described test.

Two subsequent tests simulate faults in phases B and C of lines no. 2 and no. 3, respectively. Adopted fault instant in this case is $7T/6$ and R_f is 15 Ω. As can be seen from Fig. 9, upon the occurrence of a fault, direction indicator detects a fault in phase B of line no.2 since $\mathrm{id}_{a2} > 0$, $\mathrm{id}_{b2} < 0$, and $\mathrm{id}_{c2} < 0$. Similarly, the results of Fig. 10 undoubtedly point at a fault C_3 since $\mathrm{id}_{b3} > 0$, $\mathrm{id}_{a3} < 0$, and $\mathrm{id}_{c3} < 0$. Results on Fig. 10 correspond to a fault instant $2T$ and $R_f = 80$ Ω. It can be noticed that even at high impedance fault the relays trip correctly.

Further, the network was modified, and all outgoing feeders were opened, just like feeder no. 2 in the first configuration. Now all currents are dominantly capacitive, and this case corresponds to Section 3.1. Three separate phase-to-earth faults in phases A, B, and C of lines no. 1, 2 and 3, respectively have been simulated. An earth-fault of phase A in line no. 1 (A_1) occurs at instant $4T/3$ with fault resistance of 25 Ω, an earth-fault of phase B in line no. 2 (B_2) at instant $3T/2$ with fault resistance of 100 Ω (high (impedance fault), while an earth-fault of phase C in line no. 3 (C_3) occurs at instant T with fault resistance of 1 Ω. The minimal adjusted phase current, $I_{\min}$, for changing the tripping conditions is set to 30 A, since the idle operation current of the whole network is around 10 A ($U_f \omega C_{0\mathrm{sum}} = 5.77 \cdot 10^3 \cdot 2\pi \cdot 50 \cdot 5.05 \cdot 10^{-6} \simeq 10$ A). According to Table 1, column 3, when measured phase current I_A becomes less than $I_{\min}$, the tripping conditions for faults A_1, B_2 and C_3 should be $\mathrm{id}_{a1} > 0$ & $\mathrm{id}_{b1} < 0$ & $\mathrm{id}_{c1} < 0$, $\mathrm{id}_{a2} < 0$ & $\mathrm{id}_{b2} > 0$ & $\mathrm{id}_{c2} < 0$ and $\mathrm{id}_{a3} < 0$ & $\mathrm{id}_{b3} < 0$ & $\mathrm{id}_{c3} > 0$, respectively. By comparing these conditions with values shown in Figs. 11–13, the validity of the algorithm for single phase-to-earth faults can be confirmed.

In the last configuration, the network was modified to simulate the network with nearly pure inductive load. These tests correspond to Section 3.2. All four outgoing feeders were loaded dominantly inductive, just like line no.4 in the first configuration ($\cos\varphi_4 = 0.15$). Simulation parameters and the faulted phases were the same as in the previous tests with pure capacitive load. The corresponding values of the variable id for the mentioned faults are shown in Figs. 14–16.

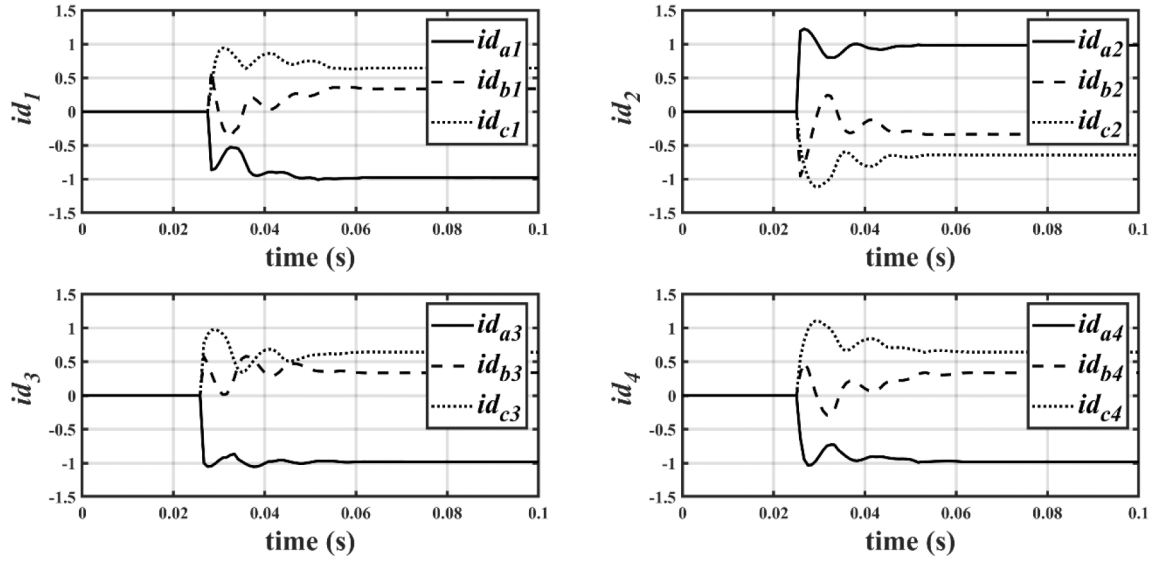

Fig. 9 *Algorithm results for a fault in phase B of line no. 2*

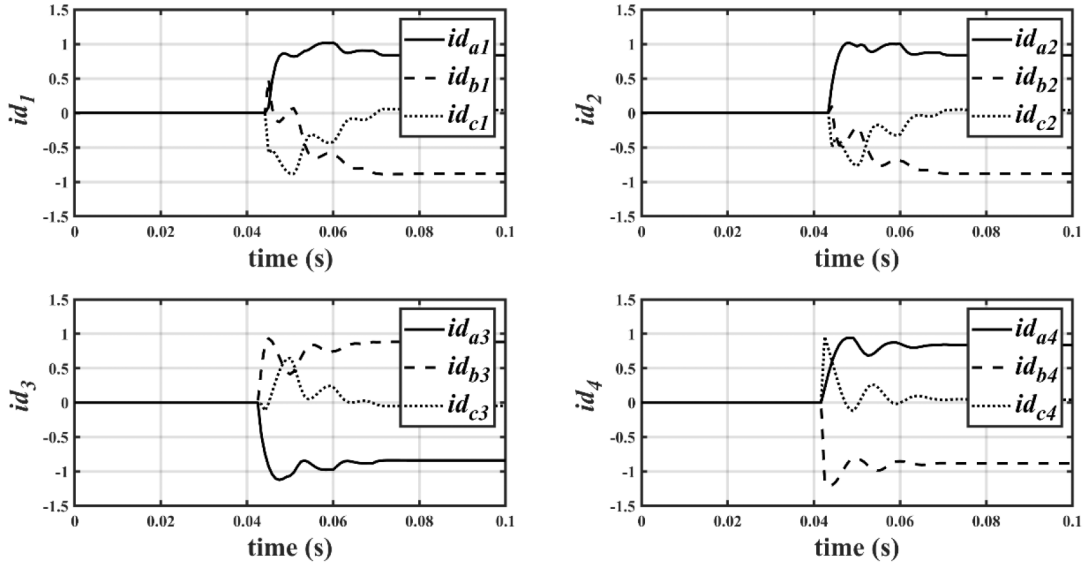

Fig. 10 *Algorithm results for a fault in phase C of line no. 3*

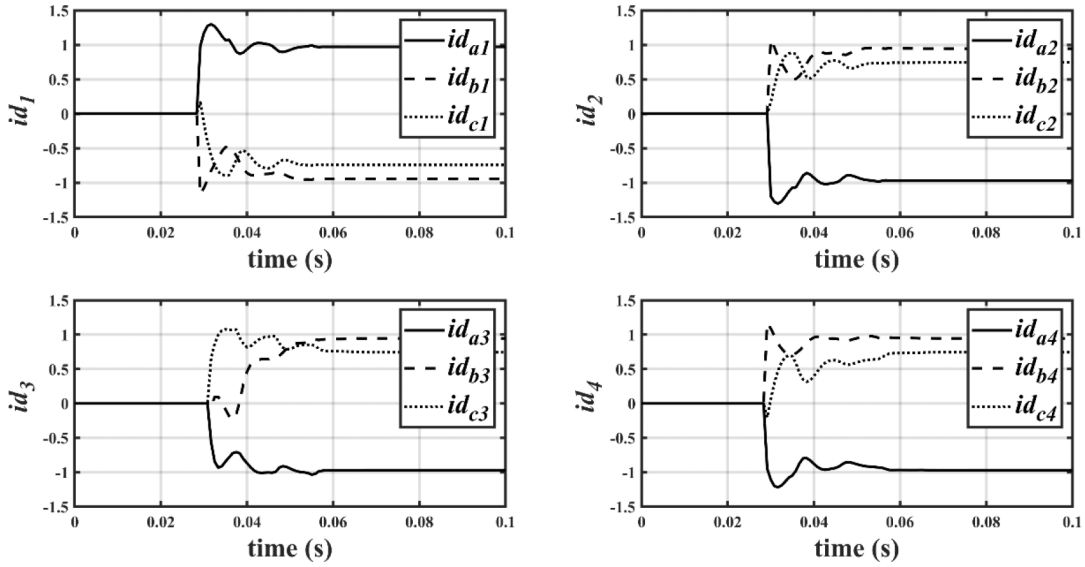

Fig. 11 *Algorithm results for a fault in phase A of line no. 1 in network with pure capacitive load*

Since the network load is extremely inductive now ($\varphi = 81.4°$) and is out of range −15° to 45°, more than one relay was triggered and the introduction of communication between them will give the appropriate output. From Fig. 14 three relays indicate phase B (B_2,

B_3, B_4), and according to column 4 of Table 1, a fault is in the phase A of the outgoing feeder where the fault has not been indicated (A_1). For example, the algorithms described in [20, 21] would in this test unselectively switch of the healthy lines 2, 3 and

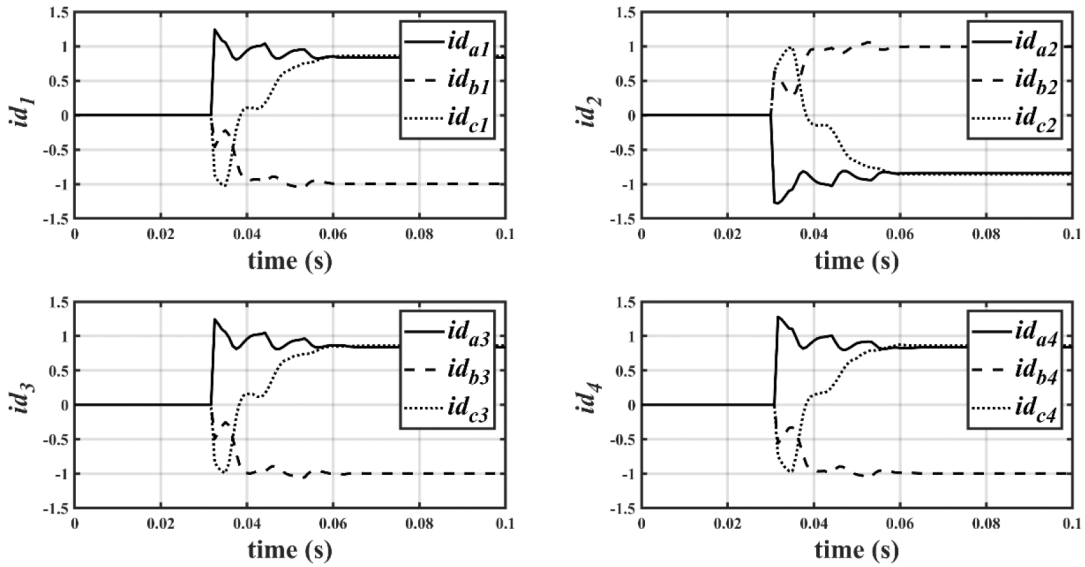

Fig. 12 *Algorithm results for a fault in B of line no. 2 in network with a pure capacitive load*

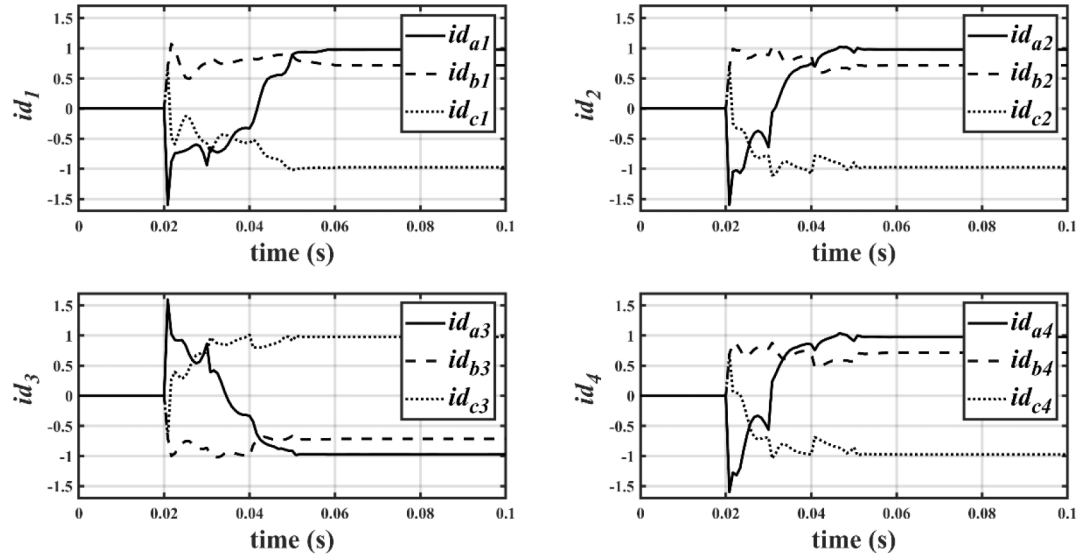

Fig. 13 *Algorithm results for a fault in phase C of line no. 3 in network with a pure capacitive load*

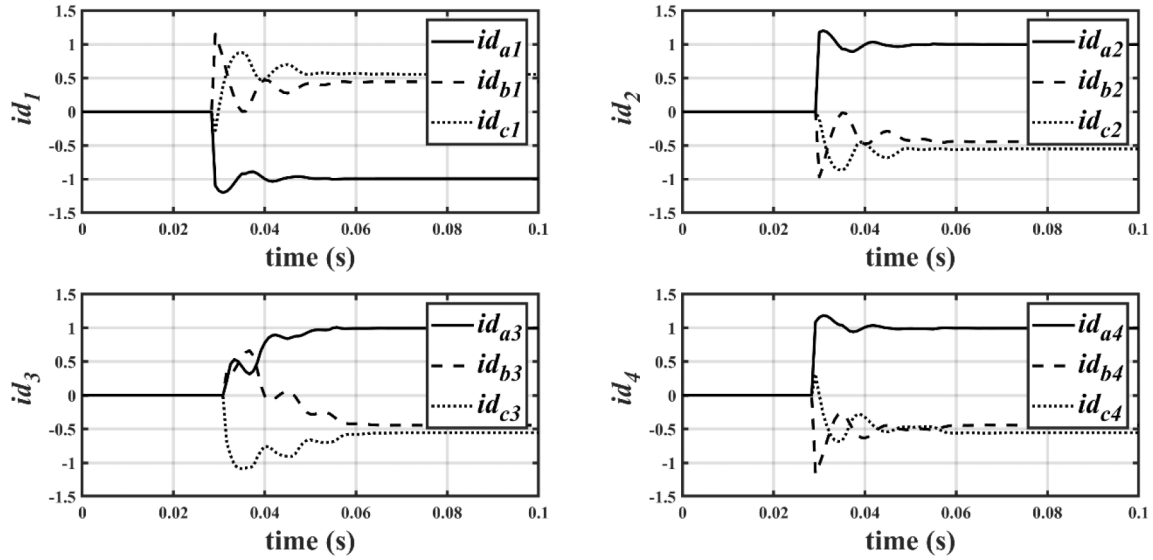

Fig. 14 *Algorithm results for a fault in phase A of line no. 1 in network with pure inductive load*

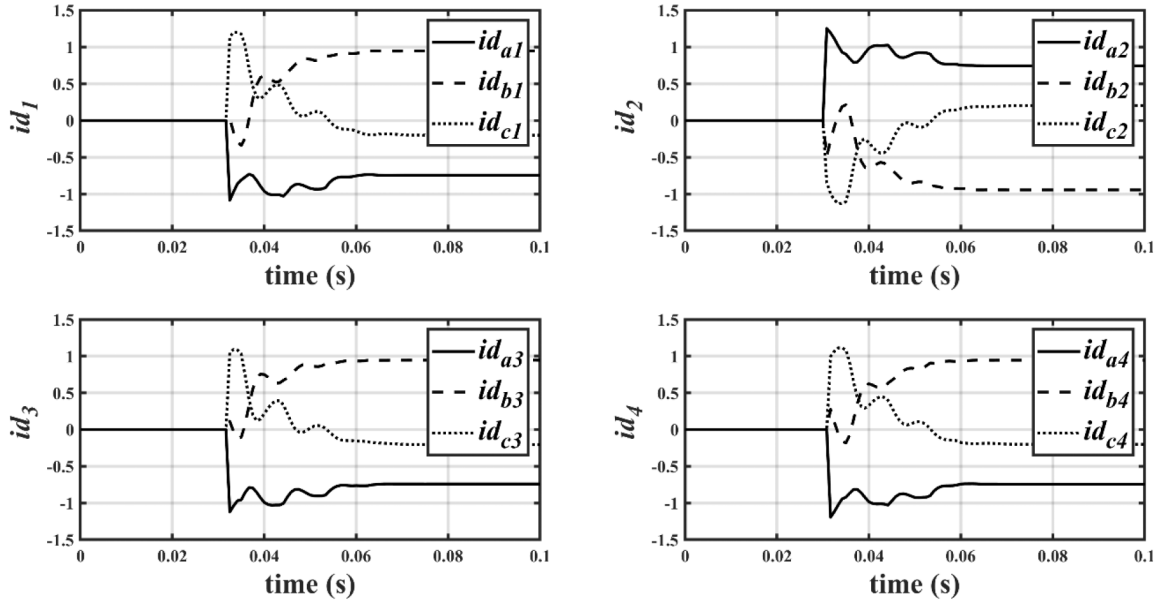

Fig. 15 *Algorithm results for a fault in phase B of line no. 2 in network with pure inductive load*

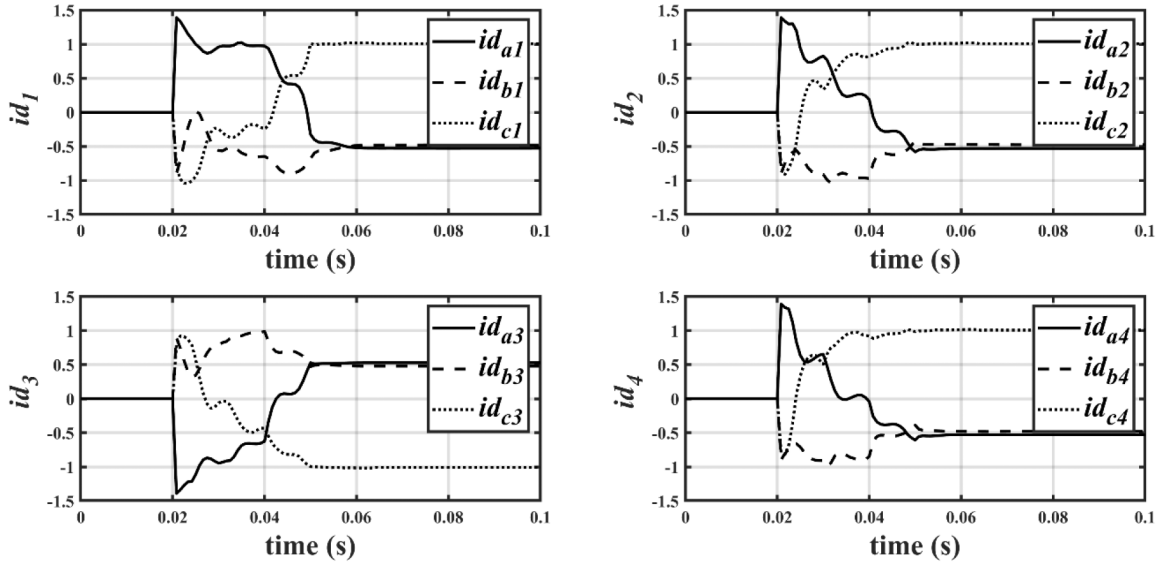

Fig. 16 *Algorithm results for a fault in phase C of line no. 3 in network with pure inductive load*

4, since the network load is outside the assumed operating range. For the same reason, these algorithms would perform incorrectly in other two tests.

From Fig. 15 three relays indicate phase C (C_1, C_3, C_4), and based on column 4 of Table 1, a fault is in phase B of the outgoing feeder where the fault has not been indicated (B_2). Similarly, from Fig. 16 three relays indicate phase A (A_1, A_2, A_4), and based on column 4 of Table 1, a fault is in phase C of the outgoing feeder where the fault has not been indicated (C_3).

As can be observed from Figs. 6–16, the response time of the relay is quite short, and it provides valid information 30 ms after the fault.

5 Conclusion

The presented algorithm is an improvement of the existing algorithms [20, 21] for overcurrent relays without voltages inputs for directional earth-fault protection in the isolated neutral system. One of the improvements is an extension of load range from 60° to 120°. Also, the number of measurements per feeder is reduced from 4 in [20], or from 2 in [21] to only 1. Using the phase current of incoming feeder as a reference quantity is more stable and less dependent on a load type of individual outgoing feeders. This approach enables not only detection of the faulted line, but also faulted phase, what conventional earth-fault protection is unable to determine. Design of these relays is undemanding and inexpensive, compared to conventional directional earth-fault relays with voltage inputs. Furthermore, the cost is additionally reduced since there is no need for voltage transformers in the substations and the required number of current measurements is reduced. The algorithm uses only simple mathematical operations for calculations, resulting in small occupation of CPU time, and can be implemented on low cost processors. Since the convergence time, including analogue and digital filtering, does not exceed 30 ms, the algorithm has an excellent response speed.

6 References

[1] Recommendations of Electric Distribution System of Serbia, Grounding of Neutral Points in Electric Distribution Networks 110 kV, 35 kV, 20 kV, 10 kV, and 0.4 kV, Technical TP-06, Belgrade, 1998

[2] Benmouyal, G., Chano, S.: 'Characterization of phase and amplitude comparators in UHS directional relays', *IEEE Trans. Power Syst.*, 1997, **12**, pp. 646–653

[3] Eissa, M.M.: 'Evaluation of a new current directional protection technique using field data', *IEEE Trans. Power Deliv.*, 2005, **20**, pp. 566–572

[4] Gan, Z., Elangovan, S., Liew, A.C.: 'Microcontroller based overcurrent relay and directional overcurrent relay with ground fault protection', *Electr. Power Syst. Res.*, 1996, **38**, pp. 11–17

[5] Benmouyal, G., Mahseredjian, J.: 'A combined directional and faulted phase selector element based on incremental quantities', *IEEE Trans. Power Deliv.*, 2001, **16**, pp. 478–484
[6] Djuric, M.B., Djurisic, Z.R.: 'Frequency measurement of distorted signals using Fourier and zero crossing techniques', *Electr. Power Syst. Res.*, 2008, **78**, pp. 1407–1415
[7] Exposito, A.G., Macias, J.A., Macias, R.J.: 'Discrete Fourier transform computation for digital relaying', *Int. J. Electr. Power Energy Syst.*, 2003, **25**, pp. 229–233
[8] Terzija, V., Djuric, M., Kovacevic, B.: 'A new self-tuning algorithm for the frequency estimation of distorted signals', *IEEE Trans. Power Deliv.*, 1995, **10**, pp. 1779–1785
[9] Terzija, V., Djuric, M.B., Jeremic, N.Z.: 'A recursive Newton type algorithm for digital frequency relaying', *Electr. Power Syst. Res.*, 1996, **36**, pp. 67–72
[10] Stojanović, Z., Djurić, M.: 'The algorithm for directional element without dead tripping zone based on digital phase comparator', *Electr. Power Syst. Res.*, 2011, **81**, pp. 377–383
[11] Chen, C.R., Lee, C.H., Chang, C.J.: 'Optimal overcurrent relay coordination in power distribution system using a new approach', *Int. J. Electr. Power Energy Syst.*, 2013, **45**, pp. 217–222
[12] Singh, M., Panigrahi, B.K., Abhyankar, A.R.: 'Optimal coordination of directional over-current relays using teaching learning-based optimization (TLBO) algorithm', *Int. J. Electr. Power Energy Syst.*, 2013, **50**, pp. 33–41
[13] Chelliah, T.R., Thangaraj, R.S., Allamsetty, M.P.: 'Coordination of directional overcurrent relays using opposition based chaotic differential evolution algorithm', *Int. J. Electr. Power Energy Syst.*, 2014, **55**, pp. 341–350
[14] Gilany, M.I., Malik, O.P., Hope, G.S.: 'A digital protection technique for parallel transmission lines using a single relay at each end', *Trans. Power Deliv.*, 1992, **7**, pp. 118–125
[15] Eissa, M.M., Malik, O.P.: 'A new digital directional transverse differential current protection', *IEEE Trans. Power Deliv.*, 1996, **11**, pp. 1285–1291
[16] Pradhan, A.K., Routray, A., Gudipalli, S.M.: 'Fault direction estimation in radial distribution system using phase change in sequence current', *IEEE Trans. Power Deliv.*, 2007, **22**, pp. 2065–2071
[17] Ashtiani, H.J., Samet, H., Ghanbari, T.: 'Simple current-based algorithm for directional relays', *IET Gener. Transm. Distrib.*, 2017, **11**, (17), pp. 4227–4237
[18] Costa, M.H., Saldanha, R.R., Ravetti, M.G., *et al.*: 'Robust coordination of directional overcurrent relays using a matheuristic algorithm', *IET Gener. Transm. Distrib.*, 2017, **11**, (2), pp. 464–474
[19] Farughian, A., Kumpulainen, L., Kauhaniemi, K.: 'Review of methodologies for earth fault indication and location in compensated and unearthed MV distribution networks', *Electr. Power Syst. Res.*, 2018, **154**, pp. 373–380
[20] Stojanović, Z., Djurić, M.: 'An algorithm for directional earth-fault relay with no voltage inputs', *Electr. Power Syst. Res.*, 2013, **96**, pp. 144–149
[21] Žarković, M., Stojanović, Z.: 'Modified algorithm for directional earth-fault protection without voltage inputs'. 2015 IEEE Eindhoven PowerTech, Eindhoven, The Netherlands July 2015